ARTICLES
PUBLISHED ONLINE: 14 SEPTEMBER 2015 | DOI: 10.1038/NMAT4408
nature materials

An electrodeposited inhomogeneous metal–insulator–semiconductor junction for efficient photoelectrochemical water oxidation

James C. Hill, Alan T. Landers and Jay A. Switzer*

The photoelectrochemical splitting of water into hydrogen and oxygen requires a semiconductor to absorb light and generate electron–hole pairs, and a catalyst to enhance the kinetics of electron transfer between the semiconductor and solution. A crucial question is how this catalyst affects the band bending in the semiconductor, and, therefore, the photovoltage of the cell. We introduce a simple and inexpensive electrodeposition method to produce an efficient n-Si/SiO_x/Co/CoOOH photoanode for the photoelectrochemical oxidation of water to oxygen. The photoanode functions as a solid-state, metal–insulator-semiconductor photovoltaic cell with spatially non-uniform barrier heights in series with a low overpotential water-splitting electrochemical cell. The barrier height is a function of the Co coverage; it increases from 0.74 eV for a thick, continuous film to 0.91 eV for a thin, inhomogeneous film that has not reached coalescence. The larger barrier height leads to a 360 mV photovoltage enhancement relative to a solid-state Schottky barrier.

Photoelectrochemical water splitting is an intriguing way to convert solar energy into a storable fuel[1,2]. Electron–hole pairs are generated and separated in the depletion region in a semiconductor electrode, and the carriers are then driven to the electrode surface to oxidize (for n-type semiconductors) or reduce (for p-type semiconductors) water. A thin catalyst layer applied to the semiconductor surface improves the kinetics of electron transfer from the semiconductor to the solution, and protects the semiconductor from photocorrosion and passivation. A fundamental question in these modified semiconductor electrodes is how this catalyst affects the band bending (and, therefore, the photovoltage) in the semiconductor[3–10]. Recent results suggest that for very thin layers of sputtered Ni on n-Si the semiconductor is not screened by the thin metal layer, and the high photovoltage is caused by the mismatch of the semiconductor/solution energetics[10]. Here, we introduce a simple and inexpensive electrodeposition method to produce an efficient n-Si/SiO_x/Co/CoOOH photoanode for the photoelectrochemical oxidation of water to oxygen gas. We also quantitatively analyse the interfacial energetics. We find that the photovoltage is determined by the catalyst, but that the barrier height for thin, inhomogeneous catalyst layers is 0.30 eV higher than the 0.61 eV that has been observed for a solid-state Schottky barrier produced in vacuum[11].

Cobalt is an earth-abundant element that becomes an efficient electrocatalyst for the oxygen-evolution reaction when oxidized to an oxide or oxyhydroxide[12–16]. It has been shown that CoO_x deposited by atomic layer deposition (ALD) onto an n-Si/p^+ junction produced by ion implantation efficiently photo-oxidizes water to oxygen in alkaline solution[17]. A large photovoltage of 0.61 V was observed in this system, which is apparently due to the buried n-Si/p^+-Si junction. A buried n-Si/p^+-Si junction was also used in a n-Si/TiO_2/Ni oxide cell produced by ALD (ref. 18). We use a simple electrodeposition method to deposit very thin layers of Co directly onto freshly HF-etched n-Si(100), without the pre-formation of a buried photovoltaic junction.

In our work, cobalt is deposited from a plating solution of 0.1 M $CoCl_2$ at pH 4 at a potential of −1.2 V versus Ag/AgCl. The optimum photoresponse and stability is observed when the Co is deposited to a charge density of 10 mC cm^{-2}. This charge density corresponds to a Faradaic thickness of 4 nm, assuming a conformal film. However, the film has not reached coalescence at a coverage of 10 mC cm^{-2}. This is shown in Fig. 1a, in which the current–time transient following a step in potential from open circuit to −1.2 V versus Ag/AgCl provides a real-time snapshot of the nucleation and growth of the film. Coverages of 10 mC cm^{-2} and 200 mC cm^{-2} are shown, respectively, as an open circle and a cross. At 10 mC cm^{-2} the current is increasing with time, consistent with an increase in area before film coalescence. Similar results were reported, in which instantaneous nucleation and growth of three-dimensional islands of Co on Si were observed[19]. Scanning electron microscope (SEM) images of the Co films on n-Si in Fig. 1b,c show that the Co grown to a coverage of 10 mC cm^{-2} has un-coalesced islands with an average size of 21 ± 8 nm, and the Co grown to a coverage of 200 mC cm^{-2} is a dense film with grains with an average size of 68 ± 25 nm. The platelets in the SEM images are $Co(OH)_2$ that is produced because of base generation owing to concomitant hydrogen evolution during the metal deposition. The analysis of the nucleation and growth current–time transients of ten films shows that film coalescence occurs at an average charge density of 34 ± 7 mC cm^{-2}. The thin, inhomogeneous Co layer which formed at 10 mC cm^{-2} is sufficient to catalyse the oxygen-evolution reaction, but is not thick enough to appreciably attenuate the incoming light (Supplementary Fig. 1). We also show that the inhomogeneous nature of the 10 mC cm^{-2} deposit may be important in maximizing the photovoltage of the cell. The Co catalyst is then activated by irradiating the n-Si/Co electrode in

Missouri University of Science & Technology, Department of Chemistry and Graduate Center for Materials Research, Rolla, Missouri 65409-1170, USA.
*e-mail: jswitzer@mst.edu

© 2015 Macmillan Publishers Limited. All rights reserved

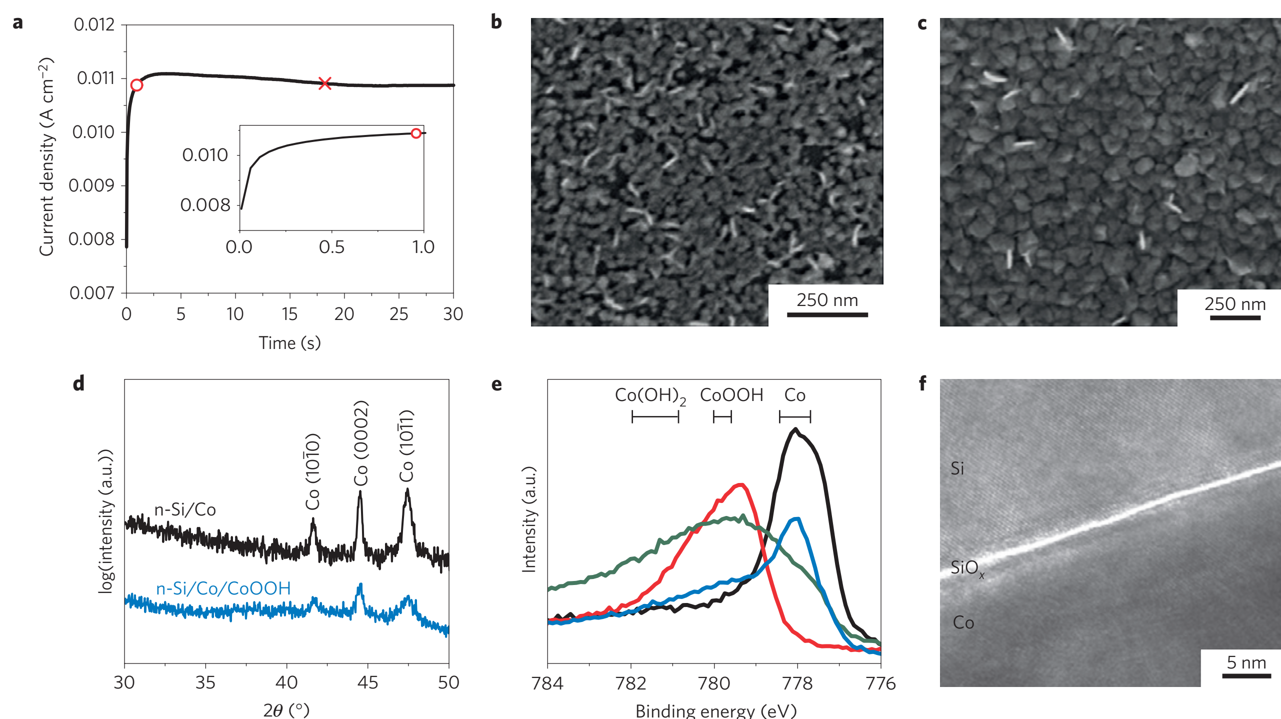

Figure 1 | Characterization of photo-oxidized electrodeposited cobalt on (100) n-Si. a, Current–time transient providing a snapshot of the nucleation and growth of Co. Charge densities of 10 mC cm^{-2} and 200 mC cm^{-2} marked with open circle and cross, respectively, for Co deposition. Inset shows the transient up to a charge density of 10 mC cm^{-2}. **b**,**c**, Scanning electron micrograph images of Co films grown to charge densities of 10 mC cm^{-2} (**b**) and 200 mC cm^{-2} (**c**). **d**, X-ray diffraction patterns of electrodeposited hexagonal cobalt before (black) and after (blue) photo-oxidation. **e**, X-ray photoelectron spectroscopy measurements of Co 2$p_{(3/2)}$ comparing as-deposited cobalt (black) and photo-oxidized cobalt that was unsputtered (red), or exposed to sputtering for 1 min (green) and 5 min (blue). The results are consistent with a layer of CoOOH on top of elemental Co. **f**, Cross-sectional TEM micrograph of the n-Si/SiO$_x$/Co/CoOOH photoanode with a coverage of 10 mC cm^{-2} after activation in 1 M KOH, showing an interfacial SiO$_x$ layer 0.5 nm thick between the n-Si and Co.

1 M KOH with 100 mW cm^{-2} simulated sunlight and scanning the potential from the open-circuit potential to 1.5 V versus Ag/AgCl until the photoresponse stabilizes.

Glancing angle X-ray diffraction (Fig. 1d) shows that the electrodeposited material is crystalline hexagonal cobalt with space group $P6_3/mmc$ (JCPDS card no. 05-0727), and that cobalt remains after the activation step. The active catalyst is CoOOH, as shown by Raman spectroscopy (Supplementary Fig. 2). Depth profiling by X-ray photoelectron spectroscopy (XPS; Fig. 1e) shows that the surface of the catalyst is Co(III), consistent with CoOOH. The XPS also shows that unreacted Co metal remains under the CoOOH, in agreement with the X-ray diffraction results. There is no evidence by XPS (Supplementary Fig. 3) for an interfacial cobalt silicide layer. Cross-sectional transmission electron microscope (TEM) analysis of the photoanodes shows that there is a layer of SiO$_x$ approximately 0.5 nm thick between the n-Si and the Co layer. The TEM image in Fig. 1f is of a photoanode with 10 mC cm^{-2} of Co after three hours of photo-oxidation at 0.5 V versus Ag/AgCl at 100 mW cm^{-2} in 1 M KOH. The SiO$_x$ layer is apparently formed when the Si wafer is inserted in the deposition solution, because it is also present on an electrode that was not irradiated, and on the photoanode with 200 mC cm^{-2} Co coverage. We have found from analysing several samples that this SiO$_x$ layer thickness can vary from 0.5 to 2 nm (Supplementary Fig. 4).

The Co-modified Si is fairly active for the oxygen-evolution reaction. Electrochemical analysis of degenerate p-silicon (p$^+$-Si) and p$^+$-Si/SiO$_x$/Co/CoOOH in 1 M KOH shows that bare p$^+$-Si is not active towards water oxidation in the relevant potential range, but p$^+$-Si/SiO$_x$/Co/CoOOH has an onset potential of about 0.5 V versus Ag/AgCl (Supplementary Fig. 5). An overpotential of only 400 mV is required to evolve oxygen at a current density of 1 mA cm^{-2}. The Tafel plot for the anode has an exchange current density of 7.24×10^{-10} A cm^{-2} based on the geometric area, and a Tafel slope of 61 mV dec^{-1} (Supplementary Fig. 5). The Tafel slope provides information about the water oxidation reaction mechanism, and is consistent with literature values in basic electrolytes that suggest an electrochemical pre-equilibrium step (oxidation of Co(III) to Co(IV)) followed by the rate-determining step (formation of O–O bond)[20].

Photoelectrochemical water oxidation on n-silicon coated with 10 mC cm^{-2} of cobalt was conducted at a light intensity equivalent to sunlight in 1 M KOH. The photoanode reaches a limiting current density of 35 mA cm^{-2} at only about 0.5 V versus Ag/AgCl under 100 mW cm^{-2} AM 1.5 irradiation (Fig. 2a). A chopped light voltammogram is shown in Supplementary Fig. 6. The photoanode is very stable in borate buffer at pH 9, but begins to decay rapidly after a few hours in 1 M KOH (Supplementary Fig. 7). Although the mechanism for the photocurrent decay is not completely understood, it seems to be due either to the dissolution of CoOOH in strong base, or to the oxidation of additional Co to CoOOH, which then exfoliates from the electrode owing to the large volume change. A similar decay in current is observed for a thin (10 mC cm^{-2}) film of Co deposited onto Au-coated glass (Supplementary Fig. 7). Electron microscope analysis of the n-Si/SiO$_x$/Co/CoOOH photoanode shows that the density of Co/CoOOH on the electrode surface is lower and the interfacial SiO$_x$ layer is thicker after device failure (Supplementary Fig. 8).

The photoelectrochemical response shown in Fig. 2a can be recast in the form of a conventional photovoltaic cell by defining the photovoltage at each current density as the difference in potential

© 2015 Macmillan Publishers Limited. All rights reserved

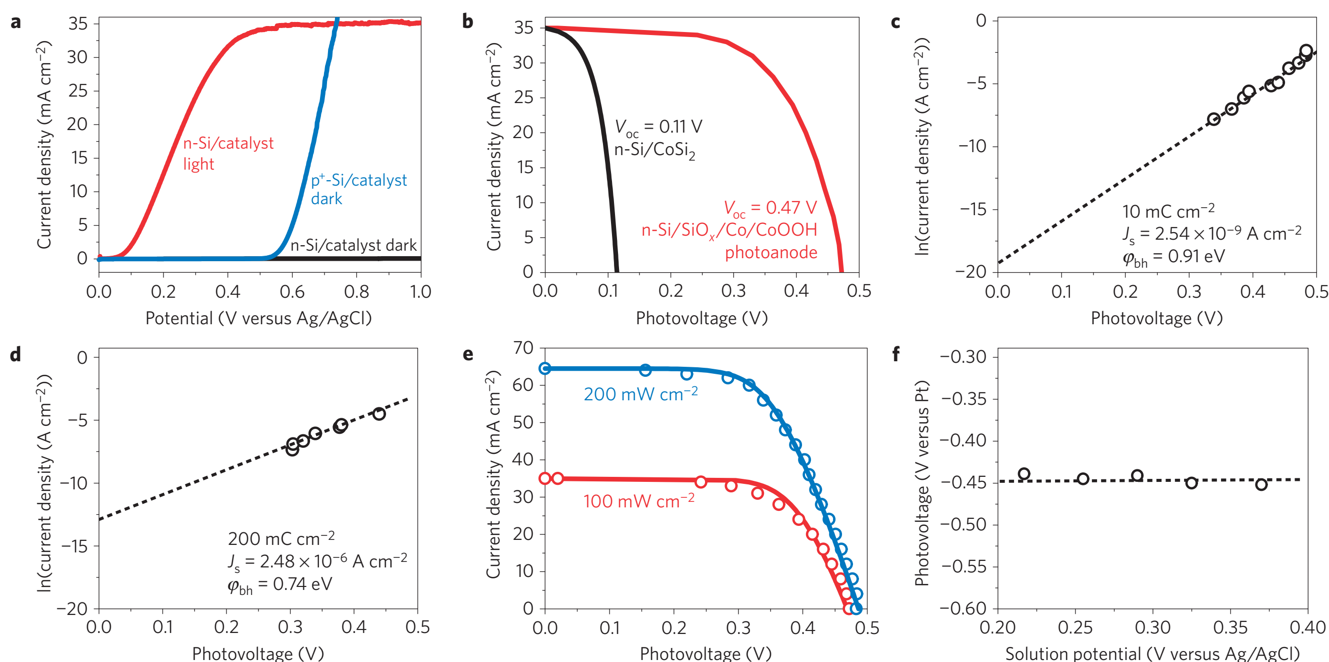

Figure 2 | Photoelectrochemical performance of the n-Si/SiO$_x$/Co/CoOOH photoanode. a, Linear sweep voltammetry comparing n-Si in the dark (black), p$^+$-Si/SiO$_x$/Co/CoOOH in the dark (blue) and n-Si/SiO$_x$/Co/CoOOH under 100 mW cm^{-2} AM 1.5 irradiation (red) in 1 M KOH at a 10 mV s^{-1} scan rate. **b**, Calculated photoresponse of an n-Si/Co Schottky cell with a barrier height of 0.61 eV (black), and measured photoresponse of the n-Si/SiO$_x$/Co/CoOOH photoanode under 100 mW cm^{-2} AM 1.5 irradiation (red). **c**,**d**, ln(J)-V plots collected by measuring the limiting photocurrent and photovoltage of photoanodes at different light intensities for photoanodes with 10 mC cm^{-2} (**c**) and 200 mC cm^{-2} (**d**) cobalt. **e**, Measured (circles) and simulated (solid line) photoresponse of the photoanode under 100 mW cm^{-2} (red) and 200 mW cm^{-2} (blue) AM 1.5 irradiation in 1 M KOH using equation (1) and values of J_s and n measured in **c** for the photoanode with 10 mC cm^{-2} Co. **f**, Measured photovoltage for 10 mC cm^{-2} photoanode in a 1 M KOH electrolyte with a series of potassium hexacyanoferrate(II) and potassium hexacyanoferrate(III) concentrations under 100 mW cm^{-2} AM 1.5 irradiation. The open-circuit photovoltage is independent of the solution potential.

between that observed in a p$^+$-Si/SiO$_x$/Co/CoOOH electrode in the dark and the irradiated n-Si/SiO$_x$/Co/CoOOH photoanode. The photovoltaic response of the electrode is shown in red in Fig. 2b. The cell has an open-circuit photovoltage of 0.47 V, short-circuit photocurrent of 35 mA cm^{-2}, fill factor of 0.62 and conversion efficiency of 10.2%. Note that this potentiostatic efficiency is the energy saved relative to the same oxygen-evolution catalyst in the dark. If the efficiency is calculated using the thermodynamic potential for water oxidation (that is, +0.204 V versus Ag/AgCl), the fill factor is 0.15 and the efficiency is 0.4% (Supplementary Fig. 9 and Supplementary Equations 1 and 2).

The question we would like to address in this study is whether the observed 0.47 V photovoltage for the photoanode is brought about by a mismatch between the Fermi level of the semiconductor and the potential of the solution due to the porous nature of the Co deposit, or to the solid-state junction. We can calculate the response of a solid-state n-Si/Co Schottky diode using the diode equation (equation (1)),

$$J = J_s(\exp^{q(V-JR_sA)/nkT} - 1) - J_L \quad (1)$$

where V is the voltage (V), n is the diode quality factor, k is Boltzmann's constant (1.38×10^{-23} J K^{-1}), T is the temperature (294 K), q is the charge of an electron (1.60×10^{-19} C), J is the observed current density (A cm^{-2}), J_s is the dark saturation current density (A cm^{-2}), J_L is the limiting current density (A cm^{-2}), R_s is the series resistance (Ω), and A is the area (cm^2; ref. 21). The barrier height, φ_{bh} (eV), can be calculated from the dark saturation current (equation (2)),

$$\varphi_{bh} = \frac{kT}{q}\ln\left(\frac{A^*T^2}{J_s}\right) \quad (2)$$

where A^* is the effective Richardson's constant (120 A cm^{-2} K^{-2} for n-Si; ref. 21). The barrier height has been measured to be 0.61 eV for an epitaxial n-Si/CoSi$_2$ Schottky barrier produced in vacuum[11]. The disilicide forms in vacuum, when there is no intervening SiO$_x$ layer. This measured barrier height for the solid-state Schottky barrier is smaller than expected on the basis of the work function of Co, because a large number of surface states in the Schottky barrier are known to lead to Fermi level pinning[22]. The simulated response of the solid-state Schottky barrier is shown in black in Fig. 2b. The calculated V_{oc} of the n-Si/CoSi$_2$ Schottky barrier is only 0.11 V, compared with the measured photovoltage of 0.47 V for the n-Si/Co/CoOOH photoanode in alkaline solution.

We can also use equation (3) (which is derived from equation (1) by letting $J = 0$)

$$V_{oc} = \frac{nkT}{q}\ln\left(\frac{J_L}{J_s}+1\right) \approx \frac{nkT}{q}\ln\left(\frac{J_L}{J_s}\right) \quad (3)$$

to determine both n and J_s for our photoanode in solution[21]. The open-circuit voltage, V_{oc}, is determined as a function of the limiting current density, J_L, in Fig. 2c,d at a series of light intensities. The thin and thick Co layers give different results. A diode quality factor, n, of 1.1 is determined from the slope of a plot of ln(J_L) versus V_{oc}, and a dark saturation current density, J_s, of 2.54×10^{-9} A cm^{-2} is determined from the intercept for the junction with 10 mC cm^{-2} Co. The dark saturation current corresponds to a barrier height of 0.91 eV, considerably larger than the 0.61 eV expected for an n-Si/CoSi$_2$ Schottky barrier formed in a vacuum. The junction produced with a thicker (200 mC cm^{-2}) layer of Co has a barrier height of 0.74 eV, and the diode quality factor is 2.0 (Fig. 2d). Figure 2e shows simulated photoresponse curves

© 2015 Macmillan Publishers Limited. All rights reserved

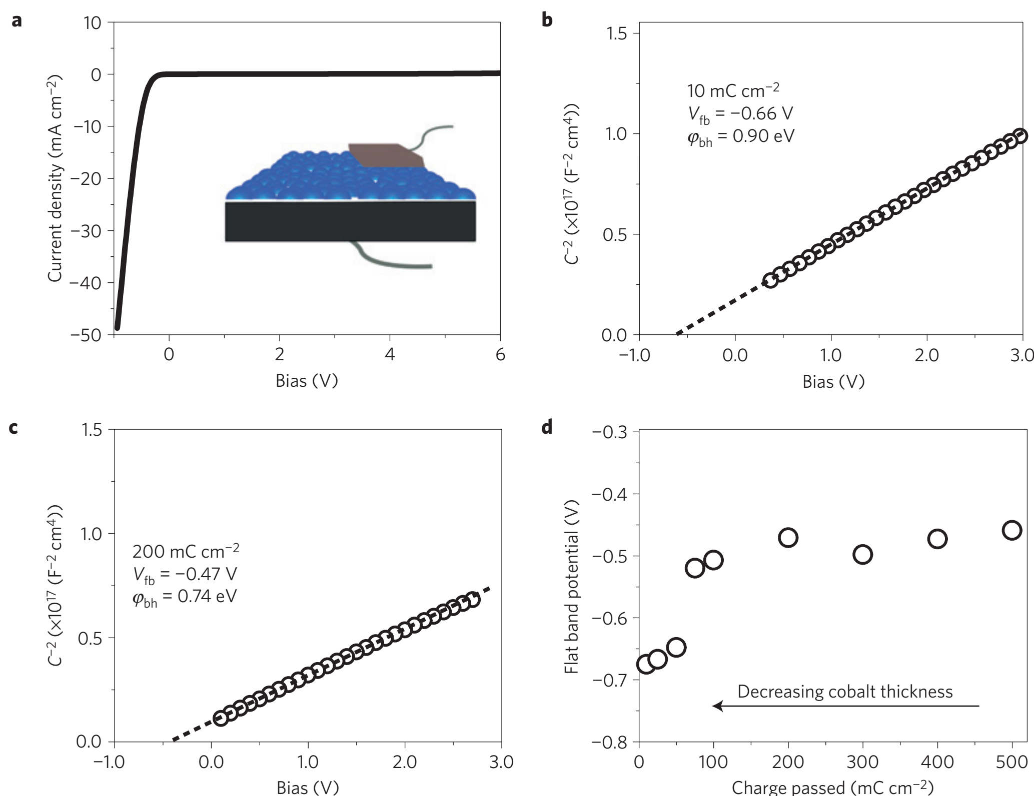

Figure 3 | Solid-state characterization of the electrodeposited n-Si/SiO$_x$/Co junction. a, Current–voltage response of n-Si/SiO$_x$/Co solid-state cell with an In front contact at a 10 mV s^{-1} scan rate showing diode behaviour. Inset shows schematic of the solid-state cell. **b**,**c**, Solid-state Mott–Schottky plots collected at reverse bias with a frequency of 100 kHz and scan rate of 10 mV s^{-1}, showing barrier heights (φ_{bh}) of 0.90 eV and 0.74 eV, respectively, for n-Si coated with 10 mC cm^{-2} (**b**) and 200 mC cm^{-2} (**c**). **d**, Flat band potentials of solid-state cells as a function of cobalt coverage determined by Mott–Schottky plots collected at a 10 mV s^{-1} scan rate and 100 kHz frequency. The flat band potential increases as the Co layer thickness decreases. At the lower Co coverages, the Co has not coalesced into a dense film.

for the photoanode with 10 mC cm^{-2} Co at 100 mW cm^{-2} and 200 mW cm^{-2} irradiances using equation (1) and the measured values of J_s, and n. A series resistance of 1.5 Ω gave the best fit to the observed data (shown as open circles in Fig. 2e). These results suggest that the photoanode does not function like a simple solid-state Schottky barrier. The two possibilities at this point are either that the Co layer is so thin and porous that it does not effectively screen the semiconductor from the solution, or that surface states are diminished at the photoanode so that Fermi level pinning is minimized. In agreement with the latter explanation, the diode quality factor of 1.1 is consistent with a low concentration of recombination sites in the bandgap of the semiconductor. Also, the photovoltage is independent of the solution potential. This was shown by measuring the open-circuit photovoltage of the photoanode versus a Pt electrode in 1 M KOH as a function of solution potential by varying the relative concentrations of potassium hexacyanoferrate(II) and potassium hexacyanoferrate(III). The photovoltage was 0.45 V regardless of solution potential (Fig. 2f). This open-circuit voltage agrees well with the measured photovoltage of 0.47 V for the water-splitting cell, suggesting that the photovoltage is controlled by the electrodeposited junction instead of the solution potential. However, the photovoltage is higher than would be expected for a simple solid-state Schottky barrier.

The interfacial energetics of the electrodeposited photoanodes were also probed by direct solid-state measurements. Pressed indium wire or silver paste front contacts yielded barrier height values independent of the material used for the front contact. The test geometry is shown as an inset to Fig. 3a. The J–V plot in Fig. 3a shows the expected rectifying behaviour of a diode with negligible dark current to a reverse bias of 6 V. Capacitance measurements in the reverse bias region were used to determine the flat band voltage. Again, the thin and thick Co layers gave different results. The Mott–Schottky plot for the 10 mC cm^{-2} Co film in Fig. 3b is linear to a reverse bias of 3 V. The x-intercept of the Mott–Schottky plot gives a flat band voltage of 0.66 V (Fig. 3b and Supplementary Equation 3). The thicker Co layer gives a flat band voltage of 0.47 V (Fig. 3c). The barrier heights can then be calculated from the flat band voltage using V_n, the difference in energy between the Fermi level and the conduction band. Using the measured carrier density (N_D) of 1.8×10^{15} cm^{-3} (Supplementary Equation 4) and the density of states in the conduction band (N_C) of 2.8×10^{19} cm^{-3}, V_n is calculated to be 0.24 eV (equation (4); ref. 21).

$$V_n = kT\ln\left(\frac{N_C}{N_D}\right) \quad (4)$$

Thus, the barrier height is 0.90 eV for the thin Co layer and 0.74 eV for the thicker Co layer. The thickness dependence of the barrier height was determined by running Mott–Schottky plots for a series of n-Si/SiO$_x$/Co junctions with cobalt thicknesses ranging from 10 mC cm^{-2} to 500 mC cm^{-2} (Fig. 3d). The n-Si/SiO$_x$/Co junctions with the thinnest cobalt layers had a barrier height about 0.2 eV greater than those formed with the thickest cobalt layers. The transition in barrier height was nearly coincident with the charge density at which film coalescence occurs (that is, 34 ± 7 mC cm^{-2}).

There seem to be two contributions to the enhanced photovoltage of the electrodeposited photoanode relative to a simple solid-state

© 2015 Macmillan Publishers Limited. All rights reserved

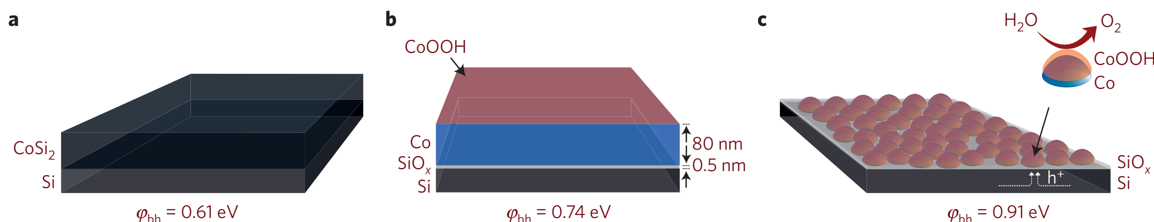

Figure 4 | Schematic of solid-state Schottky barrier and electrodeposited n-Si/SiO_x/Co/CoOOH junctions. a, Solid-state, epitaxial n-Si/$CoSi_2$ Schottky barrier produced in vacuum with 0.61 eV barrier height (φ_{bh}; ref. 11). **b**, Electrodeposited n-Si/SiO_x/Co/CoOOH junction of thick Co layer (200 mC cm^{-2}) with a barrier height of 0.74 eV. **c**, Electrodeposited n-Si/SiO_x/Co/CoOOH junction of thin, inhomogeneous Co layer (10 mC cm^{-2}) with a barrier height of 0.91 eV. The photogenerated holes are collected at the Co/CoOOH islands where they oxidize water to oxygen gas.

Schottky barrier—a thin adventitious tunnel junction of SiO_x that minimizes surface states, and inhomogeneous barrier heights for the photoanodes with thin Co layers. Because we have characterized a series of photoanodes with varying Co coverages, we can determine the contributions from each of these effects. These effects are summarized in Fig. 4, which shows schematics of the solid-state Schottky barrier and electrodeposited photoanodes with thick and thin Co layers. An interfacial SiO_x layer of tunnelling dimensions is known to cause photovoltage enhancement in metal–insulator–semiconductor (MIS) solar cells compared with Schottky barrier cells by decreasing the density of surface states[22,23]. If the density of surface states is sufficiently high, the Fermi level will be pinned by the surface states, and the barrier height typically reaches a value only two-thirds of the maximum barrier height[24]. However, if the density of surface states decreases sufficiently to cause the junction to be unpinned, the barrier height will approach the difference between the electron affinity of the semiconductor and the work function of the metal. We estimate the density of surface states to be 5.1×10^{12} states cm^{-2} eV^{-1} (Supplementary Equation 5; ref. 22). If the interfacial oxide layer is too thick, the maximum short-circuit current density will begin to decrease; this is known to occur for layers thicker than 2 nm (refs 23,24). The interfacial SiO_x layer explains why the photoanode with the thick Co layer (Fig. 4b) has a barrier height of 0.74 eV, compared with the value of 0.61 eV for a Schottky barrier formed in vacuum (Fig. 4a)[11]. The electrodeposited photoanode functions like an MIS diode with a thick, continuous metal layer.

The barrier height is further increased to 0.91 eV for photoanodes with nanometre-scale Co three-dimensional islands that have not reached coalescence (Fig. 4c). We attribute this further enhancement to the inhomogeneous nature of the MIS barrier heights. That is, the SiO_x layer is covered with nanoscale regions with different barrier heights. It has been shown by other workers that spatially non-uniform barrier height contacts in which the size of the contact is small compared with the depletion width in the semiconductors can have anomalous barrier heights due to a 'pinch-off' effect[25–27]. This has been observed both in the solid-state[25] and in photoelectrochemical cells[26,27]. We cannot rule out that the large barrier height regions of the photoanode are due to contact of the solution with the Si/SiO_x interface, but the fact that the solution and the solid-state measurements give nearly identical barrier heights suggests that this is not the case. Also, as shown in Fig. 2f, the photovoltage of the photoanode with 10 mC cm^{-2} is independent of the solution potential. A more likely explanation for the high barrier height regions is that the CoOOH layer that forms on the outside of the nanometre-scale Co islands (see, Fig. 4c) acts like a high work function contact. This argument is consistent with previous results by other workers that showed that electrodeposited Schottky barriers can have higher barrier heights than barriers formed by vapour deposition[28,29]. The enhanced barrier height of electrodeposited n-GaAs/Cu Schottky barriers has been attributed to oxidation of the electrodeposited, polycrystalline Cu contact[29].

Although the initial goal of our work was to produce a uniform catalyst layer that both catalysed the oxygen-evolution reaction and prevented SiO_x passivation of the Si surface, our studies show that a thin interfacial layer of SiO_x of tunnelling dimensions actually serves to increase the photovoltage relative to a solid-state Schottky barrier produced in vacuum. The photovoltage is further enhanced if the Co layer is non-continuous. We attribute this further enhancement to the nanoscale Co/CoOOH (core/shell) deposits that create inhomogeneous barrier heights. The n-Si/SiO_x/Co/CoOOH photoanode functions like an inhomogeneous MIS solid-state solar cell in series with an electrochemical water-splitting cell. Photogenerated holes are harvested at the Co/CoOOH islands to oxidize water to oxygen gas, as shown in Fig. 4c, similar to the 'nanoemitter' concept introduced in ref. 30. Although the electrodeposited photoanode may not have the long-term stability of electrodes produced by techniques such as ALD (refs 17,18), it produces a large photovoltage without the need for a pre-formed buried junction. The electrodeposited photoanode has an abrupt junction that does not require a thermal diffusion or ion implantation step, and should be amenable for use in solar cells based on less-expensive polycrystalline or multicrystalline silicon[7]. Electrodeposition is not only simple and inexpensive, but it may produce structures not accessible in ultrahigh vacuum.

Methods

Methods and any associated references are available in the online version of the paper.

Received 15 May 2014; accepted 27 August 2015;
published online 14 September 2015

References

1. Lewis, N. S. & Nocera, D. G. Powering the planet: Chemical challenges in solar energy utilization. *Proc. Natl Acad. Sci. USA* **103,** 15729–15735 (2006).
2. Walter, M. G. *et al.* Solar water splitting cells. *Chem. Rev.* **110,** 6446–6473 (2010).
3. Lin, F. & Boettcher, S. W. Adaptive semiconductor/electrocatalyst junctions in water-splitting photoanodes. *Nature Mater.* **13,** 81–86 (2014).
4. Gamelin, D. R. Water splitting: Catalyst or spectator? *Nature Chem.* **4,** 965–967 (2012).
5. Guo, L. *et al.* Tunnel barrier photoelectrodes for solar water splitting. *Appl. Phys. Lett.* **97,** 063111 (2010).
6. Esposito, D. V., Levin, I., Moffat, T. P. & Talin, A. A. H_2 evolution at Si-based metal–insulator–semiconductor photoelectrodes enhanced by inversion channel charge collection and H spillover. *Nature Mater.* **12,** 562–568 (2013).
7. Switzer, J. A. The n-silicon/thallium(III) oxide heterojunction photoelectrochemical solar cell. *J. Electrochem. Soc.* **133,** 722–728 (1986).
8. Chen, Y. W. *et al.* Atomic layer-deposited tunnel oxide stabilizes silicon photoanodes for water oxidation. *Nature Mater.* **10,** 539–544 (2011).
9. Fan, F.-R. F., Keil, R. G. & Bard, A. J. Semiconductor electrodes. 48. Photooxidation of halides and water on n-silicon protected with silicide layers. *J. Am. Chem. Soc.* **105,** 220–224 (1983).
10. Kenney, M. J. *et al.* High-performance silicon photoanodes passivated with ultrathin nickel films for water oxidation. *Science* **342,** 836–840 (2013).

© 2015 Macmillan Publishers Limited. All rights reserved

11. Lauwers, A. *et al.* Electrical transport in (100)$CoSi_2$/Si contacts. *J. Appl. Phys.* **77,** 2525–2536 (1995).
12. Reece, S. Y. *et al.* Wireless solar water splitting using silicon-based semiconductors and earth-abundant catalysts. *Science* **334,** 645–648 (2011).
13. Subbaraman, R. *et al.* Trends in activity for the water electrolyser reactions on 3*d* M(Ni,Co,Fe,Mn) hydr(oxy)oxide catalysts. *Nature Mater.* **11,** 550–557 (2012).
14. Koza, J. A., Hull, C. M., Liu, Y.-C. & Switzer, J. A. Deposition of β-$Co(OH)_2$ films by electrochemical reduction of tris(ethylenediamine)cobalt(III) in alkaline solution. *Chem. Mater.* **25,** 1922–1926 (2013).
15. Marsh, D. A. *et al.* Water oxidation using a cobalt monolayer prepared by underpotential deposition. *Langmuir* **29,** 14728–14732 (2013).
16. Young, E. R., Costi, R., Paydavosi, S., Nocera, D. G. & Bulović, V. Photo-assisted water oxidation with cobalt-based catalyst formed from thin-film cobalt metal on silicon photoanodes. *Energy Environ. Sci.* **4,** 2058–2061 (2011).
17. Yang, J. *et al.* Efficient and sustained photoelectrochemical water oxidation by cobalt oxide/silicon photoanodes with nanotextured interfaces. *J. Am Chem. Soc.* **136,** 6191–6194 (2014).
18. Hu, S. *et al.* Amorphous TiO_2 coatings stabilize Si, GaAs, and GaP photoanodes for efficient water oxidation. *Science* **344,** 1005–1009 (2014).
19. Munford, M. L., Sartorelli, M. L., Seligman, L. & Pasa, A. A. Morphology and magnetic properties of Co thin films electrodeposited on Si. *J. Electrochem. Soc.* **149,** C274–C279 (2002).
20. Gerken, J. B. *et al.* Electrochemical water oxidation with cobalt-based electrocatalysts from pH 0–14. The thermodynamic basis for catalyst structure, stability, and activity. *J. Am. Chem. Soc.* **133,** 14431–14442 (2011).
21. Sze, S. *Physics of Semiconductor Devices* 2nd edn (Wiley-Interscience, 1981).
22. Card, H. C. & Rhoderick, E. H. Studies of tunnel MOS diodes I. Interface effects in silicon Schottky diodes. *J. Phys. D: Appl. Phys.* **4,** 1589–1601 (1971).
23. Ng, K. K. & Card, H. C. A comparison of majority- and minority-carrier silicon MIS solar cells. *IEEE Trans. Electron. Dev.* **27,** 716–724 (1980).
24. Cowley, A. M. & Sze, S. M. Surface states and barrier height of metal–semiconductor systems. *J. Appl. Phys.* **36,** 3212–3220 (1965).
25. Tung, R. T. Electron transport at metal–semiconductor interfaces: General theory. *Phys. Rev. B* **45,** 13509–13523 (1992).
26. Nakato, Y., Ueda, K., Yano, H. & Tsubomura, H. Effect of microscopic discontinuity of metal overlayers on the photovoltages in metal-coated semiconductor-liquid junction photoelectrochemical cells for efficient solar energy conversion. *J. Phys. Chem.* **92,** 2316–2324 (1988).
27. Rossi, R. C. & Lewis, N. S. Investigation of the size-scaling behavior of spatially nonuniform barrier height contacts to semiconductor surfaces using ordered nanometer-scale nickel arrays on silicon electrodes. *J. Phys. Chem. B* **105,** 12303–12318 (2001).
28. Reineke, R. & Memming, R. High barrier GaAs/metal Schottky junctions produced by electrochemical metal deposition. *Surf. Sci.* **192,** 66–80 (1987).
29. Vereecken, P. M., Vanalme, G. M., Van Meirhaeghe, R. L., Cardon, F. & Gomes, W. P. Electrochemical reduction vs. vapour deposition for n-GaAs/Cu Schottky-barrier formation: A comparative study. *J. Chem. Soc. Faraday Trans.* **92,** 4069–4075 (1996).
30. Lewerenz, H. J. Operational principles of electrochemical nanoemitter solar cells for photovoltaic and photoelectrocatalytic applications. *J. Electroanal. Chem.* **662,** 184–195 (2011).

Acknowledgements

This material is based on work supported by the US Department of Energy, Office of Basic Energy Sciences, Division of Materials Sciences and Engineering, under Grant No. DE-FG02-08ER46518.

Author contributions

J.C.H. and A.T.L. prepared the samples and performed all measurements. J.C.H. and J.A.S. wrote the manuscript. J.A.S. directed the research.

Additional information

Supplementary information is available in the online version of the paper. Reprints and permissions information is available online at www.nature.com/reprints. Correspondence and requests for materials should be addressed to J.A.S.

Competing financial interests

The authors declare no competing financial interests.

© 2015 Macmillan Publishers Limited. All rights reserved

Methods

Materials and synthesis. Phosphorus-doped (100) n-silicon wafers with a measured resistivity of 2.3 Ω cm (Virginia Semiconductor) were cleaned by sonicating for 10 min each in ethanol and deionized water. Subsequently, the native oxide of the n-Si wafers was dissolved by submersing in 5 mM HF immediately before use. Degenerate boron-doped (100) p-silicon (p^+-Si) with 0.001–0.005 Ω cm resistivity (Virginia Semiconductor) was prepared likewise. An ohmic back contact on n-silicon was prepared with gallium–indium eutectic. A silver wire was attached to the ohmic back contact with silver paste (GC Electronics, Silver Print II) and coated with Type W wax (Apiezon) to prevent contact with the electrolyte. Cobalt was electrodeposited from an argon-purged plating solution of 0.1 M cobalt chloride (Sigma-Aldrich, 98%) in deionized water. A potential of −1.2 V versus Ag/AgCl was applied at room temperature until an appropriate charge density was passed. For solid-state measurements, a front contact was prepared by pressing indium wire (Sigma-Aldrich, 99.999%), or by coating with silver paste.

Photoelectrochemistry measurements. An Oriel LCS-100 lamp, 100 W xenon ozone-free, was used as the light source with an air mass (AM) 1.5 filter; and calibrated with a thermopile (The Eppley Laboratory). The photoelectrochemical cell consisted of 1 M potassium hydroxide (Sigma-Aldrich, 90%) as the electrolyte, an Ag/AgCl reference electrode, platinum wire as the counter electrode, and the n-Si/SiO_x/Co/CoOOH photoanode. Stability measurements were performed with 200 r.p.m. stirring. The borate buffer at pH 9 was prepared with 0.7 M boric acid (Sigma-Aldrich, 99.5%) and 0.3 M potassium hydroxide. The limiting current density of the n-Si/SiO_x/Co/CoOOH photoanode for the potentiostatic stability measurements was 27 mA cm^{-2} in 1 M potassium hydroxide and 13.5 mA cm^{-2} in borate buffer at pH 9. The applied potentials were 1 V versus Ag/AgCl in 1 M KOH and 1.3 V versus Ag/AgCl in pH 9 borate buffer. The electrolytes for measuring the effect of solution potential on photovoltage contained 1 M potassium hydroxide with 0.05, 0.20, 0.50, 0.80, or 0.95 M of potassium hexacyanoferrate(II) and 0.95, 0.80, 0.50, 0.20, or 0.05 M of potassium hexacyanoferrate(III).

© 2015 Macmillan Publishers Limited. All rights reserved